DETICKT IT: A Machine Learning-Based Application for Real-Time Tick Identification and Spatiotemporal Disease Risk Assessment

Antonia Kolb
Harvard College '28

There is an alarming increase in the population of ticks and tick-borne diseases (TBDs), with 475,000 cases reported annually, some of which are fatal. Due to limited training, healthcare providers and the public cannot always accurately identify ticks and their associated infections, leading to delayed diagnoses and treatments. Additionally, the prevalence rates of different disease-causing pathogens vary based on geographic locations. To facilitate the identification process and provide an expedited risk assessment of TBDs, a machine learning-based iOS application, DETICKT IT was created. The app features a ResNet50V2 (transfer learning) deep convolutional neural network (CNN) built in Python for combining real-time tick-species identification with a location-based tick-risk assessment by embedding the Centers for Disease Control and Prevention's (CDC's) spatiotemporal tick and pathogen surveillance statistics. With DETICKT IT, users can now receive an immediate and accurate analysis to determine whether they are at risk of contracting a certain TBD. The app is able to accurately identify the ten most common tick species in North and South America: American dog tick (*Dermacentor variabilis, D. similis*), Asian longhorned tick (*Haemaphysalis longicornis*), Brown dog tick (*Rhipicephalus sanguineus*), Eastern blacklegged tick (*Ixodes scapularis*), Western blacklegged tick (*Ixodes pacificus*), Groundhog tick (*Ixodes cookei*), Gulf Coast tick (*Amblyomma maculatum*), Lone star tick (*Amblyomma americanum*), Rocky Mountain wood tick (*Dermacentor andersoni*), and soft tick (*Ornithodoros*). The overall accuracy is 97% with precision, recall, and F1 score metrics of 0.96, 0.97, and 0.96, respectively. This freely accessible app shows promise in assisting tick bite victims with their decision to seek further medical assistance, particularly those with underlying health conditions.

Introduction

The Centers for Disease Control and Prevention (CDC) reported that 50,000 people are diagnosed with tick-borne diseases (TBDs) in the United States each year, including Lyme Disease (LD; Marx et al., 2021). However, underreporting discovered by Kugeler et al. (2021) suggests that the real incidence rate is much higher, closer to ~500,000. Due to underdiagnosis and asymptomatic clinical manifestations (Madison-Antenucci et al., 2020; Lantos et al., 2020), the scope of this public health threat is difficult to assess (Welc-Falęciak et al., 2023). Moreover, in recent decades, the number of cases has doubled, in part due to climate change (Campbell-Lendrum et al., 2023).

Ticks are ectoparasites and their range and tick-borne pathogens are increasing worldwide, with warmer winters in certain regions (Odgen et al., 2021; Kilpatrick et al., 2017) leading to phenological changes (MacDonald et al., 2019; Newman et al., 2018). While LD caused by Borrelia burgdorferi sensu stricto (Burgdorfer et al., 1982) remains one of the most prevalent tick-borne pathogens in North America, Europe, and Asia (Kugeler et al., 2015; Grochowska et al., 2020), other diseases have emerged and become pervasive in recent decades (Eisen et al., 2017). Madison-Antenucci et al. (2020) reports that the foci of endemicity or new locations of ticks is expanding and so are the pathogens and bacteria being transmitted which vary greatly by species.

The Eastern blacklegged tick (Ixodes scapularis) is one of the most clinically important ticks in the United States and abroad due to its transmission of diverse pathogens (Tokarz et al., 2019), such as Anaplasma phagocytophilum (anaplasmosis), Babesia microti (babesiosis), Borrelia miyamotoi (hard tick relapsing fever), Borrelia mayonii (LD), and Ehrlichia muris eauclairensis (ehrlichiosis; Eisen & Eisen, 2018). Other important ixodid vectors include the Asian Longhorned tick (Haemaphysalis longicornis; Egizi et al., 2020), Brown dog tick (Rhipicephalus sanguineus; Little et al., 2022), American dog tick (Dermacentor variabilis, D. similis; Newman et al., 2018), Eastern blacklegged tick (I. scapularis; Eisen et al., 2018), Lone star tick (Amblyomma americanum; Thangamani et al., 2023), Gulf Coast tick (A. maculatum; Paddock & Goddard, 2015), Groundhog tick (I. cookei; Ferreira et al., 2023), Western blacklegged tick (I. pacificus; MacDonald et al., 2019), Rocky Mountain wood tick (D. andersoni; Ebel et al., 2023), and soft tick (Ornithodoros; Chitimia-Dobler et al., 2023). These species have been associated with certain TBDs, including B. mayonii (transmitted by the I. scapularis / pacificus), B. miyamotoi (I. scapularis / pacificus), tick-borne encephalitis (TBE), Crimean-Congo hemorrhagic fever (R. sanguineus), human granulocytic anaplasmosis (HGA) caused by Anaplasma phagocytophilum (I. scapularis / pacificus), babesiosis (I. scapularis / pacificus), human monocytic ehrlichiosis (A. americanum, D. variabilis), severe fever with thrombocytopenia (SFTS; H. longicornis), Heartland virus disease (A. americanum), E. ewingii infection (A. americanum), Powassan encephalitis (I. scapularis / cookei), and Bourbon virus disease (A. americanum; Madison-Antenucci et al., 2020). Tick exposure and bites are also associated with other diseases and co-infections (Lantos et al., 2020), such as Rocky Mountain Spotted Fever (RMSF; Dahlgren et al., 2017), Southern Tick-Associated Rash Illness (STARI; Belisle et al., 2017), Alpha-Gal Syndrome (AGS; Karim, et al., 2019), a red-meat allergy

associated with bites from the Lone star tick (A. americanum), Gulf Coast tick (A. maculatum), American dog tick (D. variabilis, D. similis), and Eastern blacklegged tick (I. scapularis), among other TBDs (Madison-Antenucci et al., 2020). The Asian longhorned tick (H. longicornis), indigenous to Asia (Beard et al., 2018), has recently been associated with the transmission of thrombocytopenia syndrome (SFTS) and viral hemorrhagic fevers (VHFs; Luo et al., 2015), Rickettsia japonica [Japanese spotted fever (JSF); Mahara, 1997], Anaplasma, Babesia, Borrelia, Ehrlichia, and Rickettsia (Beard et al., 2018).

Despite existing antibiotic treatments, diseases such as LD can become chronic if not treated immediately (Eisen et al., 2017). Moreover, LD affects more than two million people in the U.S. (DeLong et al., 2019), with many cases remaining undiagnosed due to atypical clinical manifestations or the absence of an otherwise characteristic "erythema migrans" skin rash (Nathavitharana & Mitty, 2015). Moreover, the economic burden of TBDs and LD is significant – estimated between $345 million and $968 million per year – with an average of $1,200 per treatment, and with later stages of disease development being more costly (Hook et al., 2022). Thus, there is a need for diagnostic capabilities to be improved, and machine learning-based approaches may offer potential solutions (Rich et al., 2022; Akbarian et al., 2021; Omodior et al., 2021; Sanchez-Galan et al., 2023).

The pathogens and diseases transmitted are dependent upon both the tick species and the geographical location of the tick; therefore, the classification of the tick species is critical to formulating an accurate diagnosis (Otranto et al., 2012). Traditional diagnostic methods have used tick species classification to inform whether a person is at risk of contracting a TBD, primarily LD (Nieto et al., 2018). However, there is no direct correlation between a certain species of tick and the TBD that the species carries, since the risk factors vary greatly for both tick lifecycle and geographic location (James et al., 2006; Madison-Antenucci et al., 2020). Clinical studies of patients presenting with a tick bite in Lyme-endemic areas have shown that the prevalence of LD in all species of ticks fluctuates, including the notorious biting arachnid Eastern blacklegged tick (I. scapularis). Moreover, Poland et al., (2001) concluded that the abundance of host-seeking infected ticks is not linearly correlated with the probability of disease transmission of the LD spirochete Borrelia burgdorferi sensu stricto (Eisen et al., 2016). Rather the proportion of ticks infected with B. burgdorferi s.s. informed the risk of human LD infection (Hinckley et al. 2016). With this degree of uncertainty, it is necessary to couple real-time identification with location-specific incidence rate data. Connecting these datasets in one platform is beneficial, since the general public and healthcare professionals alike find tick recognition challenging due to the large number of different species known and intra-species variability (Madison-Antenucci et al., 2020). Thus, morphological identification of tick species is imperative for accurate TBD risk assessment (Nieto et al., 2018). Moreover, some ticks are often difficult to identify using only morphological traits because of the allopatric nature of certain species (Chilton et al., 2013), and thus the geographic location of the ticks can inform the probability of species (Riggs et al., 2015).

Correct identification requires in-depth entomological training due to feature-wise minute differences that are difficult for the general public to identify (Nieto et al., 2018). Computer vision-based approaches to tick identification have been successful, with Rich et al. (2022) creating a convolutional neural network (CNN) that can accurately identify the American dog tick (D. variabilis, D. similis), Eastern blacklegged tick (I. scapularis), and the Lone star tick (A. americanum) with 99.5% accuracy on a given test dataset when transfer learning is used. Other deep learning algorithms feature the three major human-biting tick species (Akbarian et al., 2021; Omodior et al., 2021) with the highest reported accuracy of 93% (Sanchez-Galan et al., 2023). These machine learning-based approaches can proficiently classify images as noted in multiple studies where deep learning models were implemented for insect identification (Rich et al., 2022).

Given that human experts are the limiting factor for diagnostic capacity in this field as well as the pressing health concerns over TBDs worldwide, deep learning-based models hold promise for the instantaneous assessment of TBD risks based on specimen determination and prevalence analytics.

Materials and Methods

Project Overview

The goal of this project was to create a machine learning-based mobile application that could be used to identify the species of a tick and provide disease risk analysis based on the location of the user. The three most pathogenic ticks are the Eastern blacklegged tick (I. scapularis), Lone star tick (A. americanum), and American dog tick (D. variabilis, D. similis) and were thus used in previous versions of this study. After fine-tuning the model and adjusting the hyperparameters, ten species in total were identified: American dog tick (D. variabilis, D. similis), Asian longhorned tick (H. longicornis), Brown dog tick (R. sanguineus), Eastern blacklegged tick (I. scapularis), Western blacklegged tick (I. pacificus), Groundhog tick (I. cookei), Gulf Coast tick (A. maculatum), Lone star tick (A. americanum), Rocky Mountain wood tick (D. andersoni), and soft tick (Ornithodoros; **Fig. 1**).

For the first iteration of the system, a learning model that could accurately identify the aforementioned three most disease-producing tick species was created. Inception v3 (a CNN) was used in a previous version of the app, reaching an accuracy of 80%; however, after closer examination, the model was overfitting and misclassifying ticks and non-ticks. Thus, a different CNN, Xception, was

Figure 1. A taxonomic representation of the ten species used for tick identification. Photos of the American dog tick (*D. variabilis, D. similis*), Asian longhorned tick (*H. longicornis*), Brown dog tick (*R. sanguineus*), Eastern blacklegged tick (*I. scapularis*), Western blacklegged tick (*I. pacificus*), Groundhog tick (*I. cookei*), Gulf Coast tick (*A. maculatum*), Lone star tick (*A. americanum*), Rocky Mountain wood tick (*D. andersoni*), and soft tick (*Ornithodoros*) are featured.

chosen to detect whether a tick was present or not as well as determine the species of tick. After fine-tuning the subsequent version of the model that could identify ten species, a risk assessment was created based on the CDC's U.S. tick-borne surveillance data. For user accessibility, an iOS mobile application with other useful features was deployed onto the Apple App Store.

Validation, Testing, Dataset Preparation, and Data Preprocessing

For the three-species-model, a dataset was curated. To collect the image sets, web scrapers were utilized to collect photos of each class of ticks from readily available datasets on Google Images, iNaturalist, and other image platforms. Manual cleaning of noise and removing photos of mislabeled species was implemented to ensure the dataset used was morphologically correct (**Fig. 1**). Most images were also from databases that genetically confirmed their species classification using molecular assays (Luo et al., 2022). Images were then cropped and resized to 500 ppx to prevent object (tick) occlusion. The cleaned dataset included 3,123 photos: 776 "non-ticks," 743 American dog ticks, 807 Eastern blacklegged ticks, and 797 Lone star ticks. Each class equally represented 25% of the set, and model weights were adjusted accordingly to balance the set.

After the three-species model was built, the training, validation, and testing datasets were built for the ten-species neural network. This dataset featured 709 "non-ticks," 579 American dog ticks, 849 Blacklegged ticks, 809 Lone Star ticks, 409 Brown Dog ticks, 612 Rocky Mountain ticks, 644 Gulf Coast ticks, 683 Asian longhorned ticks, 780 Groundhog ticks, and 312 soft ticks **(Fig. 1)**. Of note, the Eastern and Western blacklegged tick were combined into one class, because the features were too similar for a neural network to differentiate, and hence a heuristic algorithm was applied which will be discussed later. For classes such as soft ticks where there was a lack of available photos, the class weights were adjusted to compensate for imbalance and impact during the training process.

The data pipeline for both iterations was comparable. To prevent data leakage between classes, a two-step dataset split process was performed. The first split divided the dataset into training, validation, and testing subsets. The second split, exclusively applies data augmentation to the training set and splits the rest of the dataset into training, validation, and testing. Following the data preprocessing and pre-cropping to 500 ppx, data augmentation was implemented to increase the data variability by creating three copies of all the photos each with different orientations. The testing set was isolated from the training pipeline to safeguard against data contamination and biased model performance evaluation. By presenting the testing data, or the "unseen" and new data, to the model, the unbiased performance could be evaluated.

Ticks are very small ranging from 3-5 mm; therefore, their varying appearances are difficult to detect by the human eye as well as for some neural networks (Rich et al., 2022). The Xception model is known for its ability to pick up small features (Chollet, 2017), however, small ticks were originally a challenging task. To overcome this problem, tiny black squares were placed on the data set to generate noise and enable the model to pay closer attention to minor feature changes, such as color, distinctive dots and shapes, and tick shape (**Fig. 2**). After applying the black dots, the model showed an ability to generalize, which was later used for the ten ticks.

Figure 2. Sample selection of photos of female and male *I. scapularis, A. americanum, D. variabilis, D. similis,* and a "Non-tick" class that were used for training with the "Black Dot" method. Black dots were used to induce noise and allow model generalization.

Model Architecture and Selection

For the task of tick image classification, a CNN was chosen (Rich et al., 2022). The architecture of the model, however, would be crucial to the performance, so different CNNs were tested and compared for different iterations and number of species detected as well as their computational efficiency and ability to generalize.

The models tested were ResNet50V2, ResNet152V2 (an improvement of ResNet50), and Xception. ResNet50V2, from the ResNet architecture (He et al., 2016), has a 50-layer deep architecture that is able to identify shortcut connections to improve gradient flow and ease of training. It is often pre-trained on large datasets to employ transfer learning, allowing it to be suitable for complexity and performance. ResNet152V2 is more complex than ResNet50V2 with a 152-layer deep architecture. It is also often used for transfer learning due to its pre-trained weights. Xception, or "Dense Extreme Inception," builds on the Inception architecture and replaces traditional convolutions with depth-wise separable convolutions for better feature extraction (Chollet, 2017).

Each model was trained for 10 epochs or periods of time, and the performances were compared (**Fig. 3-5**). ResNet50V2 ended with a loss of 0.2225 (**Fig. 3A**) and accuracy of 0.922 (**Fig. 3B**). The model performed well across the loss and accuracy metrics, however, the high testing and validation accuracy indicated the model was overfitting on the training and validation datasets, while not performing well on the test dataset. ResNet152V2 ended with a loss of 0.3125 (**Fig. 4A**) and an accuracy of 0.844 (**Fig. 4B**). Similar to ResNet50V2, the training and validation sets displayed high accuracy, the test set did not perform well. Last, Xception was tested, ending with a loss of 0.2708 (**Fig. 5A**) and accuracy of 0.8937 (**Fig. 5B**). Unlike the other models tested, Xception performed well and was not overfitting as seen in the consistency of the training, validation, and testing accuracy metrics. The dotted line, denoting the testing accuracy, was around the training and validation accuracy (**Fig. 5B**), while the other models' training and validation accuracies were well above the dotted line (**Fig. 3B, 4B**).

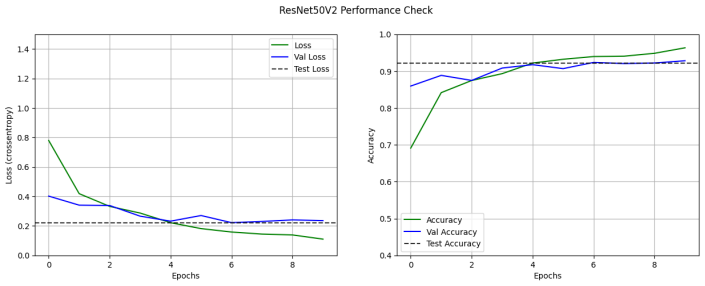

Figure 3. Model performance of ResNet50V2. **A)** Train, Validation, and Test loss metrics. **B)** Train, Validation, and Test accuracy metrics. The dotted line is the test accuracy (B), which indicates overfitting due to the high train and validation accuracy and lower test accuracy.

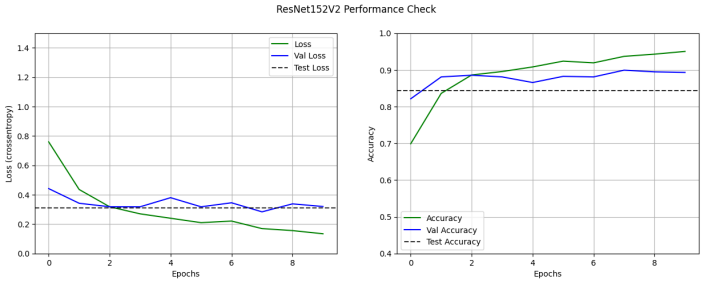

Figure 4. Model performance of ResNet152V2. **A)** Train, Validation, and Test loss metrics. **B)** Train, Validation, and Test accuracy metrics. Similar to ResNet50V2, the dotted line is the test accuracy (B), which indicates overfitting due to the high train and validation accuracy and lower test accuracy.

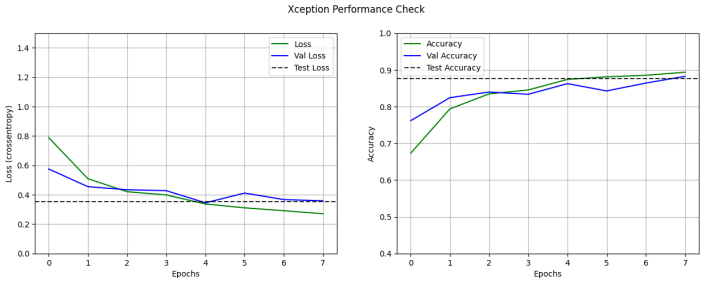

Figure 5. Model performance of Xception. **A)** Train, Validation, and Test loss metrics. **B)** Train, Validation, and Test accuracy metrics. Unlike the ResNets, Xception was not overfitting, which can be seen as the three train, validation, and test accuracy metrics are consistent.

Thus, Xception was the appropriate architecture for the tick classification CNN due to its feature extraction and depth, as seen in the model parameters (**Table 1**). The CNN consisted of multiple layers, pooling, and fully connected layers designed for the challenging task of identifying minute differences for tick species identification.

Model	Xception
Trainable parameters	21,086,252
Non-trainable parameters	54,528
Total parameters	21,140,780

Table 1. Xception model architecture and parameters for identification of three species.

While the Xception model worked well for three species, the architecture had to be reevaluated for the implementation of ten-species classification. The same networks ResNet152V2 (**Fig. 6A**), Xception (**Fig. 6B**), and ResNet50V2 (**Fig. 7B**) were tested and evaluated with the addition of MobileNetV2 (**Fig. 7A**), a lightweight architecture often used in mobile applications (Howard et al., 2017). It is resource-efficient in constrained environments, which is less relevant in this study since high accuracy is prioritized. Both ResNet152V2 and Xception are computationally intensive and have similar results (**Fig. 6A-B**) as ResNet50V2 (**Fig. 7B**). ResNet50v2, an improved version of ResNet50 (He et al., 2016), balances efficiency and performance with architectural features, pre-activation, bottleneck structures, and pre-trained weights that make it effective for feature extraction and stable training. It consistently outperformed the other models in terms of its validation accuracy and loss (**Fig. 7B**). Thus, ResNet50V2 was chosen (**Table 2**), as highlighted in **Figure 7B,** for the task of identifying the ten species due to its robust initial performance and potential for future facile fine-tuning.

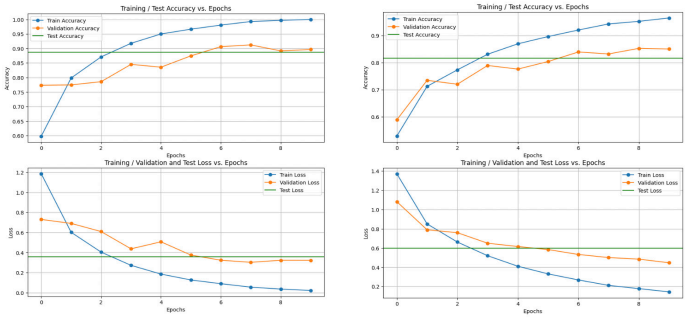

Figure 6. Model performance of ResNet152V2 and Xception. **A)** ResNet152V2 Train, Validation, and Test loss metrics. **B)** Xception Train, Validation, and Test accuracy metrics.

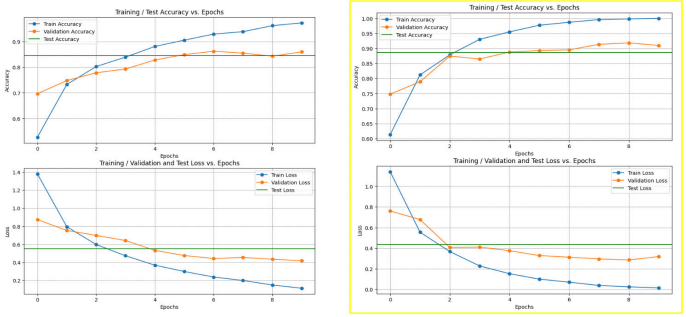

Figure 7. Model performance of MobileNetV2 and ResNet50V2. **A)** MobileNetV2 Train, Validation, and Test loss metrics of MobileNet. **B)** ResNet50V2 Train, Validation, and Test accuracy metrics.

Model	ResNet50V2
Trainable parameters	23,782,922
Non-trainable parameters	45,440
Total parameters	23,828,362

Table 2. ResNet50V2 Model Architecture and Parameters For Identification of Three Species.

Model Finetuning

After Xception was chosen for the three ticks, 13 hyperparameters, such as batch size, learning rate, and dropout rate, were adjusted to fine-tune the model in order to reach peak performance and create a robust learner, preventing the model from overfitting (**Table 1**). Similar hyperparameter optimization was implemented for the ten species with ResNet50V2 (**Table 2**) since Xception was no longer suitable as more species were added. For the ten species, the model adjustments took ~19 hours to train and ended with a validation accuracy of 97.2%.

The "Window Algorithm"

While the validation accuracy, after running the model with the test dataset, was relatively high, a collection of real-world

Figure 8. Novel Window Algorithm implementation. **A)** A zoomed-out photo was given to the model with a tiny tick surrounded by a noisy background. **B)** Model zoomed in. **C)** Model cropped again. **D)** Final cropped image that allowed for more than 95% confidence that a tick was present and the species was correct.

tick photos that the model would newly encounter yielded only an accuracy of 46%. The testing data were structurally different from the training and validation sets because they often featured occluded tick images and other realistic yet sometimes unusual user-generated photo scenarios. Most of the issues were related to the model detecting "non-tick" when, in fact, there was a tick present. To overcome this, the "window algorithm," was designed and implemented. The window algorithm continuously cropped the photo until over 95% confidence was reached by the model with regard to the species classification or whether a tick was present. If the model reached 95% confidence on a species, then the predicted class was presented to maintain computational efficiency. If the model reported over 95% confidence that there was no tick present, the window algorithm would also be run.

In **Figure 8**, the model was given a photo of a zoomed-out tick, which was a Lone star tick by its true label. When the zoomed-out photo was tested, the model predicted "non-tick" with 0.9999323 confidence (**Fig. 8A**). After running the window algorithm once, the model once again predicted "non-tick" with 0.9998989 confidence (**Fig. 8B**). The second time, the CNN predicted a "Lone star tick" with 0.7222055 confidence (**Fig. 8C**). While the model eventually predicted the true class, 72% confidence was too low to report to users. Thus, the algorithm was run again, and the CNN predicted "Lone star tick" with 0.998703 confidence (**Fig. 8D**). This demonstrated the network's ability to use real-world examples despite the small size challenge of ticks. If the model does not reach 0.95 confidence that there is a tick in the photo, the user will receive a "tick not found" notification, which allows them to re-center the tick for optimal results.

Location-Based Heuristic Algorithm Approach

While the window algorithm significantly improved the model performance for three types of ticks, as more species were added, the neural network misclassified certain types, such as the Eastern and Western blacklegged ticks, whose inter-species differences are highly refined. However, their geographic ranges are different. While all blacklegged ticks are morphologically similar feature-wise, it is rare to find an Eastern blacklegged tick in California or a Western blacklegged tick in Connecticut (Nieto et al., 2018). Utilizing the CDC's tick surveillance data by state, the probability of a certain tick found in a given geographic region could be ascertained. When the user takes a photo of a tick with the app, their geographic coordinates will be assigned to a respective state (or country if outside the U.S.).

Tick-Borne Disease Risk Assessment

Information for the spatiotemporal risk assessment was used from the CDC's Tickborne Pathogen Surveillance data. The CDC's dataset displayed the prevalence of the following vectors in the U.S. by species: LD, Tularemia, Spotted Fever Rickettsiosis (SFR), Anaplasmosis, Ehrlichia chaffeensis, E. ewingii, babesiosis, Powassan encephalitis, hard tick relapsing fever, Bourbon virus disease, and Southern Tick-Associated Rash Illness (STARI).

Of note, because of the COVID-19 pandemic (Boyce et al., 2023), some of the TBD datasets only go back to 2019; and due to lack of available data and privacy issues, the risk assessment currently works only in the U.S. and South America. The ticks most documented by the CDC are the Lone star tick, American dog tick, and the Eastern blacklegged tick. The CDC's National Notifiable Diseases Surveillance System (NNDSS) releases a dataset including pathogen prevalence by geography and displays the annual incidence of diseases in the U.S.. For example, the I. scapularis set reports the following pathogens: Borrelia burgdorferi sensu stricto (responsible for LD), B. mayonii, B. miyamotoi, Anaplasma phagocytophilum, E. muris eauclairensis (EME), Babesia microti, and the Powassan (POW) virus. Furthermore, due to the lack of information available in some areas, location-based weighting was applied to the CDC dataset based on population size and the proportion of infected individuals from tick bites to predict the risk of infection if a user in a given region is bitten. Moreover, since there is some known underreporting of cases, tick risk analysis must take into account that actual risks may inevitably be higher or lower, respectively.

For easier public use, a gradient scale from "low level" to "high level" of danger was implemented (**Fig. 9E**). However, a user of the app can also view the full risk breakdown of the pathogen prevalence by selecting "view risks," which displays more risk details associated with notifiable TBDs. Prior to taking the photo of the tick, the user fills out a form that provides ground information for their risk assessment. In the form, the user is asked if the tick has bitten someone or an animal and later asks if the tick was engorged or enlarged when found (**Fig. 9C**). The risk will only be considered "high level" if a tick bite was reported.

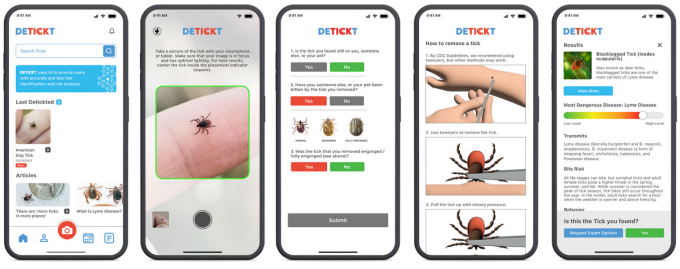

Figure 9. DETICKT IT UI / UX Schematic. **A)** The DETICKT IT homescreen where users can see ticks that they have identified. **B)** The camera feature to take the photo of the tick. **C)** After users take the photo, they will be prompted to fill out the risk background form which will further inform the risk assessment. **D)** If the user selects that they still have a tick attached, a tutorial on how to remove a tick based on CDC guidance will appear. **E)** After prior steps, the user will receive the tick species as determined, their potential risk of a tick-borne infection, and more information about the tick.

iOS Application User Interface (UI) / User Experience (UX) Design and Features

DETICKT IT was originally developed in Xcode with Swift within a service-oriented architecture. After the CNN model (Figure 7B) was ported from a local environment to Amazon Web Services (AWS), open application programming interfaces (APIs) were created for functions, such as specimen identification, location finder, and risk assessment. Using this approach, DETICKT IT is able to scale through AWS Lambda functions, thereby delivering results to the app's users in mere seconds. The code was later migrated to Flutter because it serves as a codebase for both iOS and Android – with a view toward eventually increasing availability to Android users as well.

DETICKT IT has an active "tick-bite" data pipeline, which allows users who have been bitten or are interested in the definitive identification of a tick they have found to upload their images (Figure 9). There are other features, such as a "Learn More" (Figure 9E), where users can learn about other ticks and track their symptoms after a tick bite. Figure 9 outlines the prominent features of the mobile application.

Results

Model Performance Metrics

The model was first evaluated for three species and later for ten. After using the Xception CNN and implementing the window algorithm, an accuracy of 97% was reached for the three most prevalent ticks. After optimization with the ResNet50V2 model, the accuracy for ten ticks was also 97%. Prior to implementing the window algorithm, the confusion matrices, which display the model's performance in terms of true labels versus the predicted label (**Fig. 10**), indicate few false positives and false negatives in both the validation and the test sets. However, it is important to evaluate the model with unfamiliar datasets containing images that feature partially occluded ticks and other real-world scenarios (including less-than-ideal photographic settings). This was a challenge for the model and resulted in only 46% accuracy, but the novel window algorithm provided a feasible approach to dealing with realistic, user-produced images.

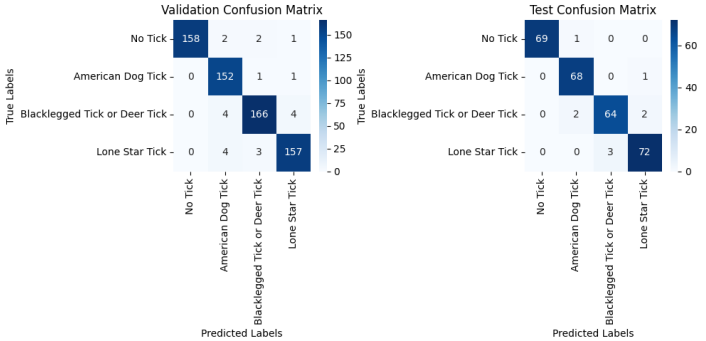

Figure 10. Test and validation confusion matrices prior to implementing the Window Algorithm. **A)** Validation and **B)** Test Confusion Matrices. The implementation of the window algorithm decreased the errors of the model due to feature-based classification.

After applying the window algorithm for N = ~45 in each class, there were only very minor classification errors (**Fig. 11**). Of note, the errors occurred when the model reported that there was no tick present when in fact there was. This indicates that the model was not confusing the species, but rather having difficulty locating the tick in the photo. Therefore, after refining the window algorithm, the accuracy of the model was increased to 97%. In one notable instance, during preprocessing, an image was misclassified by human error but was correctly identified by the model, another display of the CNN's ability to generalize.

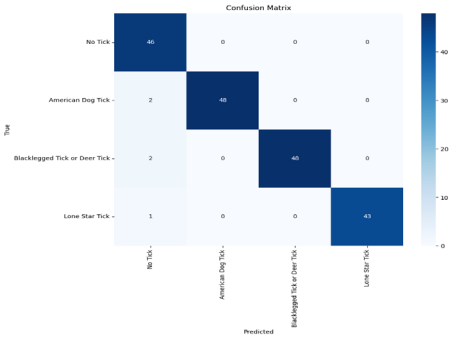

Figure 11. Confusion matrix after implementing the Window Algorithm. Minimal errors are occurring, as seen in the distribution. The model was not confusing species but rather could not always detect a tick in a photo.due to feature-based classification.

F1, accuracy, recall, and precision scores were calculated for the three ticks (**Table 3**). These reflect the model's performance and ability to generalize. The eventual model ended up performing overall with 0.98 precision, 0.97 recall, and 0.97 F1 score.

The three-species model worked well as seen in the confusion matrices (**Fig. 11**), so gradually more species were added until classification of ten species was reached. In **Figure 12**, confusion matrices for six ticks are shown. The classification report indicated that the network struggled with classifying the Rocky Mountain wood tick with only 0.47 precision. The CNN's overall performance had 84% accuracy after the addition of three new types of ticks. Due to the morphological similarities between the Rocky Mountain wood tick, the American dog tick, and the Gulf Coast tick, the aforementioned location-based heuristic algorithm was applied. This greatly increased the model's accuracy to 93% (**Fig. 12B**). **Figure 12B** is the confusion matrix post-algorithm utilization with fewer classification errors committed.

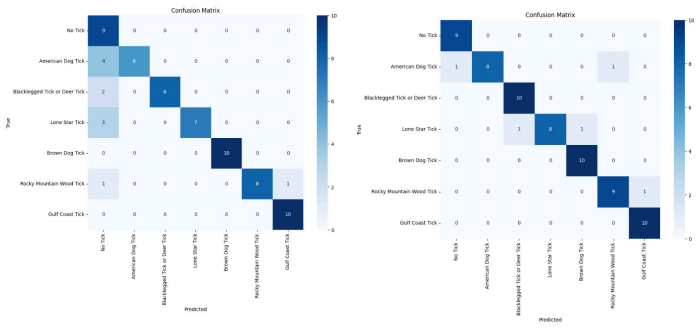

Figure 12. Confusion matrices for six ticks with Window Algorithm pre- and post-Location Heuristic Feature. **A)** Confusion matrix without the location feature. **B)** Confusion matrix post-location feature algorithm applied, greatly improving the performance of the model.due to feature-based classification.

After 93% accuracy was achieved and the location-based algorithm was used as well as after changing the model to ResNet50V2, the ten-species model was tested. While adding these three species, the Asian longhorned tick, the Groundhog tick, and the soft tick, they all had distinct features which were not challenging for the model to identify. **Figure 13** displays the validation and test confusion matrices for the ten species. There is a very minimal error rate for both matrices, which is indicative of the model's high performance (**Fig. 13**).

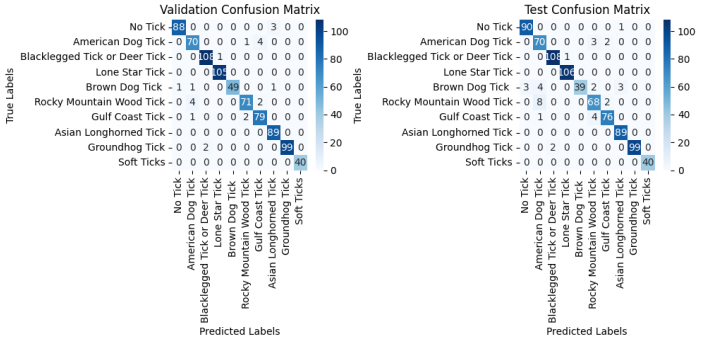

Figure 13. Confusion matrices after implementing the Window Algorithm. Minimal errors occurred, as seen in the distribution. **A)** Validation confusion matrix. **B)** Test confusion matrix.

After using random photos not contained in the training set as well as applying both the window and location algorithm, the confusion matrix in **Figure 14** was produced. There are not many classification errors, and the remaining challenges relate to interspecies similarities. Overall, the model for ten species ultimately reached an accuracy of 97%, precision of 96%, recall of 97%, and F1 score of 96%. After applying these innovative algorithms in concert, the accuracy of this latest model is exhibiting real-world viability.

Model	Precision	Recall	F1 score	Overall Accuracy
Three Species	0.98	0.97	0.97	0.97
Ten Species	0.96	0.97	0.96	0.97

Table 3. Performance Metrics of Both Models: Precision, Recall, and F1 Scores.

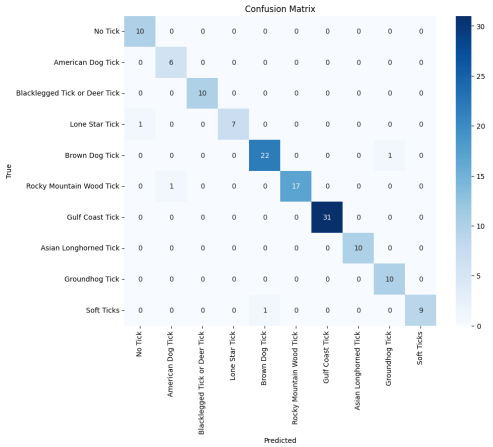

Figure 14. Confusion matrix for ten species and "non-tick" control class after implementing the Window Algorithm and Location-Based Heuristic Algorithm. Minimal errors are seen in the distribution with a relatively high true positive rate.

Discussion

The performance metrics indicate that the neural network can suitably generalize and classify ticks at a relatively more accurate (97%) and certainly faster rate than the general public (Nieto et al., 2018). The gradual expansion to ten species allowed for the meticulous optimization and refinement of the CNN architecture. Moreover, the implementation of the location-based heuristic and novel window algorithms represents an innovative approach to achieving real-world applicability and scalability. The window algorithm can also be applied to other problems, such as medical imaging (Müller et al., 2021) or computer vision tasks where minute object features are difficult to detect or discern.

While a machine learning-based approach to tick identification has been explored, this novel mobile app can identify the ten most common and disease-causing species and predict the risk posed by each tick (by connecting to the CDC's tick-borne disease prevalence database). Based on the literature, this is the first implementation of a machine learning-based app that can identify ticks with high (97%) accuracy as well as provide a qualified assessment of the potential risk of infection.

There are current limitations with the availability of data in regard to tick photos and tick-borne disease surveillance databases. Due to the lack of available data, transfer learning was also utilized to compensate for any data disparities. Future versions of the app include expanding the geographic regions to other countries (data availability permitting) to provide this service more globally to tick bite victims.

One of the most challenging aspects of tick species classification is the minute appearance differences between species. While 97% is relatively high and due to the model's reported performance, which is indicative that the network isn't overfitting, there is still uncertainty with the quality of user-produced images. Since this mobile device- and user-centric approach is highly dependent on the quality of the photos received, during training and testing, real-world scenarios of occluded, relatively blurry, and zoomed-out photos of ticks were used, yet these approaches still may not have accounted for all user-produced errors.

The risk of tick-borne diseases varies by stage of the tick and sex (Eisen et al., 2016); therefore, a viable computer vision-led approach to determining disease risk must be able to account for these differences. With certain species, the male ticks look distinct from their female counterparts – visual differences an ML model can learn to distinguish. In future iterations, the model would incorporate training a female and male class for each species, whereas at present no delineation is made between male and female species during training. Once again, accurate photographic data availability / accessibility remains a significant issue for further improving overall performance with the incorporation of this new feature.

This mobile app has the potential to significantly outperform medical professionals' reported ability to accurately classify ticks (Nieto et al., 2018). Moreover, the embedded tick risk assessment feature allows users to gain awareness of the risks associated with a given tick (bite) in a certain geographic area and in real time. The knowledge and confidence gained will facilitate diagnostic accuracy and shorten critical time-to-treatment, enabling affected individuals to seek medical attention. DETICKT IT is currently available on Apple's App Store and is free, with ~3,000 downloads (as of 09/01/24).

References

Akbarian, S., Nelder, M. P., Russell, C., Cawston, T., Moreno, L., Patel, S. N., Allen, V., & Dolatabadi, E. (2021). A Computer Vision Approach to Identifying Ticks related to Lyme Disease. *IEEE Journal of Translational Engineering in Health and Medicine*, *10*(4900308), 1–1. https://doi.org/10.1109/jtehm.2021.3137956

Arahirwa, V., Tyrlik, K., Abernathy, H., Cassidy, C. A., Alejo, A., Mansour, O., Giandomenico, D., Amanda Brown Marusiak, & Boyce, R. M. (2023). Impact of the COVID-19 pandemic on delays in diagnosis and treatment of tick-borne diseases endemic to southeastern USA. *Parasites & Vectors*, *16*(1). https://doi.org/10.1186/s13071-023-05917-8

Beard, C. B., Occi, J., Bonilla, D. L., Egizi, A. M., Fonseca, D. M., Mertins, J. W., Backenson, B. P., Bajwa, W. I., Barbarin, A. M., Bertone, M. A., Brown, J., Connally, N. P., Connell, N. D., Eisen, R. J., Falco, R. C., James, A. M., Krell, R. K., Lahmers, K., Lewis, N., & Little, S. E. (2018). Multistate Infestation with the Exotic Disease–Vector Tick Haemaphysalis longicornis — United States, August 2017–September 2018. MMWR. *Morbidity and Mortality Weekly Report, 67*(47). https://doi.org/10.15585/mmwr.mm6747a3

Binder, A., Bockmayr, M., Hägele, M., Wienert, S., Heim, D., Hellweg, K., Ishii, M., Stenzinger, A., Hocke, A., Denkert, C., Müller, K.-R., & Klauschen, F. (2021). Morphological and molecular breast cancer profiling through explainable machine learning. *Nature Machine Intelligence, 3*(4), 355–366. https://doi.org/10.1038/s42256-021-00303-4

Burgdorfer, W., Barbour, A., Hayes, S., Benach, J., Grunwaldt, E., & Davis, J. (1982). Lyme disease-a tick-borne spirochetosis? *Science, 216*(4552), 1317–1319. https://doi.org/10.1126/science.7043737

Campbell-Lendrum, D., Neville, T., Schweizer, C., & Neira, M. (2023). Climate change and health: three grand challenges. *Nature Medicine, 29*(7), 1631–1638. https://doi.org/10.1038/s41591-023-02438-w

Chollet, F. (2017). Xception: Deep Learning with Depthwise Separable Convolutions. *2017 IEEE Conference on Computer Vision and Pattern Recognition (CVPR)*. https://doi.org/10.1109/cvpr.2017.195

Crispell, G., Commins, S. P., Archer-Hartman, S. A., Choudhary, S., Dharmarajan, G., Azadi, P., & Karim, S. (2019). Discovery of Alpha-Gal-Containing Antigens in North American Tick Species Believed to Induce Red Meat Allergy. *Frontiers in Immunology, 10*. https://doi.org/10.3389/fimmu.2019.01056

Dahlgren, F. S., Holman, R. C., Paddock, C. D., Callinan, L. S., & McQuiston, J. H. (2012). Fatal Rocky Mountain Spotted Fever in the United States, 1999–2007. *The American Journal of Tropical Medicine and Hygiene, 86*(4), 713–719. https://doi.org/10.4269/ajtmh.2012.11-0453

Dantas-Torres, F., Chomel, B. B., & Otranto, D. (2012). Ticks and tick-borne diseases: a One Health perspective. *Trends in Parasitology, 28*(10), 437–446. https://doi.org/10.1016/j.pt.2012.07.003

DeLong, A., Hsu, M., & Kotsoris, H. (2019). Estimation of cumulative number of post-treatment Lyme disease cases in the US, 2016 and 2020. *BMC Public Health, 19*, 352. https://doi.org/10.1186/s12889-019-6681-9

Dergousoff, S. J., Galloway, T. D., Lindsay, L. R., Curry, P. S., & Chilton, N. B. (2013). Range Expansion of Dermacentor variabilis and Dermacentor andersoni (Acari: Ixodidae) Near Their Northern Distributional Limits. *Journal of Medical Entomology, 50*(3), 510–520. https://doi.org/10.1603/me12193

Egizi, A., Bulaga-Seraphin, L., Alt, E., Bajwa, W. I., Bernick, J., Bickerton, M., Campbell, S. R., Connally, N., Doi, K., Falco, R. C., Gaines, D. N., Greay, T. L., Harper, V. L., Heath, A. C. G., Jiang, J., Klein, T. A., Maestas, L., Mather, T. N., Occi, J. L., & Oskam, C. L. (2020). First glimpse into the origin and spread of the Asian longhorned tick, Haemaphysalis longicornis, in the United States. *Zoonoses and Public Health, 67*(6), 637–650. https://doi.org/10.1111/zph.12743

Eisen, L., & Eisen, R. J. (2016). Critical Evaluation of the Linkage Between Tick-Based Risk Measures and the Occurrence of Lyme Disease Cases: Table 1. *Journal of Medical Entomology, 53*(5), 1050–1062. https://doi.org/10.1093/jme/tjw092

Eisen, R. J., & Eisen, L. (2018). The Blacklegged Tick, Ixodes scapularis : An Increasing Public Health Concern. *Trends in Parasitology, 34*(4), 295–309. https://doi.org/10.1016/j.pt.2017.12.006

Eisen, R. J., Kugeler, K. J., Eisen, L., Beard, C. B., & Paddock, C. D. (2017). Tick-Borne Zoonoses in the United States: Persistent and Emerging Threats to Human Health. *ILAR Journal, 58*(3), 319–335. https://doi.org/10.1093/ilar/ilx005

Ferreira, F. C., González, J., Milholland, M. T., Tung, G. A., & Fonseca, D. M. (2023). Ticks (Acari: Ixodida) on synanthropic small and medium-sized mammals in areas of the northeastern United States infested with the Asian longhorned tick, Haemaphysalis longicornis. *International Journal for Parasitology*. https://doi.org/10.1016/j.ijpara.2023.06.003

Fritzsche, A., Zaenker, S., Gottwald, J., Keil, R. S., Zaenker, C., Bröker, M., & Chitimia-Dobler, L. (2023). Distribution of the soft tick Carios vespertilionis in lowlands and low mountain regions of Germany. *Experimental and Applied Acarology, 91*(1), 89–97. https://doi.org/10.1007/s10493-023-00822-2

Grant, A., Lineberry, M. W., Sundstrom, K. D., Allen, K., & Little, S. J. (2022). Geographic Distribution and Seasonality of Brown Dog Tick Lineages in the United States. *Journal of Medical Entomology, 60*(1), 102–111. https://doi.org/10.1093/jme/tjac172

Gray, J. S., & Ogden, N. H. (2021). Ticks, Human Babesiosis and Climate Change. *Pathogens, 10*(11), 1430. https://doi.org/10.3390/pathogens10111430

Grochowska, A., Milewski, R., Pancewicz, S., Dunaj, J., Czupryna, P., Milewska, A. J., Róg-Makal, M., Grygorczuk, S., & Moniuszko-Malinowska, A. (2020). Comparison of tick-borne pathogen prevalence in Ixodes ricinus ticks collected in urban areas of Europe. *Scientific Reports, 10*(1). https://doi.org/10.1038/s41598-020-63883-y

Harris, E. K., Foy, B. D., & Ebel, G. D. (2023). Colorado tick fever virus: a review of historical literature and research emphasis for a modern era. *Journal of Medical Entomology*. https://doi.org/10.1093/jme/tjad094

He, K., Zhang, X., Ren, S., & Sun, J. (2016). Identity Mappings in Deep Residual Networks. *Computer Vision – ECCV 2016*, 630–645. https://doi.org/10.1007/978-3-319-46493-0_38

Hinckley, A. F., Meek, J. I., Ray, J. A. E., Niesobecki, S. A., Connally, N. P., Feldman, K. A., Jones, E. H., Backenson, P. B., White, J. L., Lukacik, G., Kay, A. B., Miranda, W. P., & Mead, P. S. (2016). Effectiveness of Residential Acaricides to Prevent Lyme and Other Tick-borne Diseases in Humans. *Journal of Infectious Diseases, 214*(2), 182–188. https://doi.org/10.1093/infdis/jiv775

Hook, S. A., Jeon, S., Niesobecki, S. A., Hansen, A. P., Meek, J. I., Bjork, J. K. H., Dorr, F. M., Rutz, H. J., Feldman, K. A., White, J. L., Backenson, P. B., Shankar, M. B., Meltzer, M. I., & Hinckley, A. F. (2022). Economic Burden of Reported Lyme Disease in High-Incidence Areas, United States, 2014–2016 - Volume 28, Number 6—June 2022 - Emerging Infectious Diseases journal - CDC. Wwwnc.cdc.gov, 28(6). https://doi.org/10.3201/eid2806.211335

James, A. M., Burdett, C., McCool, M. J., Fox, A., & Riggs, P. (2015). The geographic distribution and ecological preferences of the American dog tick,Dermacentor variabilis(Say), in the U.S.A. *Medical and Veterinary Entomology, 29*(2), 178–188. https://doi.org/10.1111/mve.12099

James, A. M., Freier, J. E., Keirans, J. E., Durden, L. A., Mertins, J. W., & Schlater, J. L. (2006). Distribution, Seasonality, and Hosts of the Rocky Mountain Wood Tick in the United States. *Journal of Medical Entomology, 43*(1), 17–24. https://doi.org/10.1093/jmedent/43.1.17

Kilpatrick, A. M., Dobson, A. D. M., Levi, T., Salkeld, D. J., Swei, A., Ginsberg, H. S., Kjemtrup, A., Padgett, K. A., Jensen, P. M., Fish, D., Ogden, N. H., & Diuk-Wasser, M. A. (2017). Lyme disease ecology in a changing world: consensus, uncertainty and critical gaps for improving control. *Philosophical Transactions of the Royal Society B: Biological Sciences, 372*(1722), 20160117. https://doi.org/10.1098/rstb.2016.0117

Koczwarska, J., Pawełczyk, A., Dunaj-Małyszko, J., Polaczyk, J., & Welc-Falęciak,

R. (2023). Rickettsia species in Dermacentor reticulatus ticks feeding on human skin and clinical manifestations of tick-borne infections after tick bite. *Scientific Reports, 13*(1), 9930. https://doi.org/10.1038/s41598-023-37059-3

Kugeler, K. J., Farley, G. M., Forrester, J. D., & Mead, P. S. (2015). Geographic Distribution and Expansion of Human Lyme Disease, United States. *Emerging Infectious Diseases, 21*(8), 1455–1457. https://doi.org/10.3201/eid2108.141878

Kugeler, K. J., Schwartz, A. M., Delorey, M. J., Mead, P. S., & Hinckley, A. F. (2021). Estimating the Frequency of Lyme Disease Diagnoses, United States, 2010–2018. *Emerging Infectious Diseases, 27*(2), 616–619. https://doi.org/10.3201/eid2702.202731

Lantos, P. M., Rumbaugh, J., Bockenstedt, L. K., Falck-Ytter, Y. T., Aguero-Rosenfeld, M. E., Auwaerter, P. G., Baldwin, K., Bannuru, R. R., Belani, K. K., Bowie, W. R., Branda, J. A., Clifford, D. B., DiMario, F. J., Halperin, J. J., Krause, P. J., Lavergne, V., Liang, M. H., Meissner, H. C., Nigrovic, L. E., & Nocton, J. (Jay) J. (2020). Clinical Practice Guidelines by the Infectious Diseases Society of America (IDSA), American Academy of Neurology (AAN), and American College of Rheumatology (ACR): 2020 Guidelines for the Prevention, Diagnosis and Treatment of Lyme Disease. *Clinical Infectious Diseases, 72*(1). https://doi.org/10.1093/cid/ciaa1215

Luo, C.-Y., Pearson, P., Xu, G., & Rich, S. M. (2022). A Computer Vision-Based Approach for Tick Identification Using Deep Learning Models. *Insects, 13*(2), 116. https://doi.org/10.3390/insects13020116

Luo, L.-M., Zhao, L., Wen, H.-L., Zhang, Z.-T., Liu, J.-W., Fang, L.-Z., Xue, Z.-F., Ma, D.-Q., Zhang, X.-S., Ding, S.-J., Lei, X.-Y., & Yu, X. (2015). Haemaphysalis longicornis Ticks as Reservoir and Vector of Severe Fever with Thrombocytopenia Syndrome Virus in China. *Emerging Infectious Diseases, 21*(10), 1770–1776. https://doi.org/10.3201/eid2110.150126

MacDonald, A. J., O'Neill, C., Yoshimizu, M. H., Padgett, K. A., & Larsen, A. E. (2019). Tracking seasonal activity of the western blacklegged tick across California. *Journal of Applied Ecology, 56*(11), 2562–2573. https://doi.org/10.1111/1365-2664.13490

Madison-Antenucci, S., Kramer, L. D., Gebhardt, L. L., & Kauffman, E. (2020). Emerging Tick-Borne Diseases. *Clinical Microbiology Reviews, 33*(2). https://doi.org/10.1128/cmr.00083-18

Mahara, F. (1997). Japanese Spotted Fever: Report of 31 Cases and Review of the Literature. *Emerging Infectious Diseases, 3*(2), 105–111. https://doi.org/10.3201/eid0302.970203

Marx, G. E., Spillane, M., Beck, A., Stein, Z., Powell, A. K., & Hinckley, A. F. (2021). Emergency Department Visits for Tick Bites — United States, January 2017–December 2019. MMWR. *Morbidity and Mortality Weekly Report, 70*. https://doi.org/10.15585/mmwr.mm7017a2

Merchan, F., Contreras, K., Gittens, R. A., Loaiza, J. R., & Sanchez-Galan, J. E. (2023). Deep metric learning for the classification of MALDI-TOF spectral signatures from multiple species of neotropical disease vectors. *Artificial Intelligence in the Life Sciences, 3*(100071), 100071. https://doi.org/10.1016/j.ailsci.2023.100071

Minigan, J. N., Hager, H. A., Peregrine, A. S., & Newman, J. A. (2018). Current and potential future distribution of the American dog tick (Dermacentor variabilis, Say) in North America. *Ticks and Tick-Borne Diseases, 9*(2), 354–362. https://doi.org/10.1016/j.ttbdis.2017.11.012

Molins, C. R., Ashton, L. V., Wormser, G. P., Andre, B. G., Hess, A. M., Delorey, M. J., Pilgard, M. A., Johnson, B. J., Webb, K., Islam, M. N., Pegalajar-Jurado, A., Molla, I., Jewett, M. W., & Belisle, J. T. (2017). Metabolic differentiation of early Lyme disease from southern tick–associated rash illness (STARI). *Science Translational Medicine, 9*(403), eaal2717. https://doi.org/10.1126/scitranslmed.aal2717

Nathavitharana, R. R., & Mitty, J. A. (2015). Diseases from North America: focus on tick-borne infections. *Clinical Medicine, 15*(1), 74–77. https://doi.org/10.7861/clinmedicine.14-6-74

Nieto, N. C., Porter, W. T., Wachara, J. C., Lowrey, T. J., Martin, L., Motyka, P. J., & Salkeld, D. J. (2018). Using citizen science to describe the prevalence and distribution of tick bite and exposure to tick-borne diseases in the United States. *PLOS ONE, 13*(7), e0199644. https://doi.org/10.1371/journal.pone.0199644

Oghenekaro Omodior, Saeedpour-Parizi, M. R., Rahman, Md. K., Azad, A., & Clay, K. (2021). Using convolutional neural networks for tick image recognition – a preliminary exploration. *Experimental and Applied Acarology, 84*(3), 607–622. https://doi.org/10.1007/s10493-021-00639-x

Paddock, C. D., & Goddard, J. (2015). The Evolving Medical and Veterinary Importance of the Gulf Coast tick (Acari: Ixodidae). *Journal of Medical Entomology, 52*(2), 230–252. https://doi.org/10.1093/jme/tju022

Poland, G. A. (2001). Prevention of Lyme Disease: A Review of the Evidence. *Mayo Clinic Proceedings, 76*(7), 713–724. https://doi.org/10.4065/76.7.713

Reynolds, E. S., Wooldridge, J. T., Stevenson, H. L., & Thangamani, S. (2023). The Lone Star tick, Amblyomma americanum, salivary factors exacerbate the clinical outcome of Heartland virus disease in a small animal model. *Scientific Reports, 13*(1), 13304. https://doi.org/10.1038/s41598-023-40397-x

Sanchez-Vicente, S., Tagliafierro, T., Coleman, J. L., Benach, J. L., & Tokarz, R. (2019). Polymicrobial Nature of Tick-Borne Diseases. *MBio, 10*(5). https://doi.org/10.1128/mbio.02055-19

Sinha, D., & El-Sharkawy, M. (2019). Thin MobileNet: An Enhanced MobileNet Architecture. *2019 IEEE 10th Annual Ubiquitous Computing, Electronics & Mobile Communication Conference (UEMCON)*. https://doi.org/10.1109/uemcon47517.2019.8993089